Journal Name

RSCPublishing

COMMUNICATION

Switching of Electrochemical Characteristics of Redox Protein upon Specific Biomolecular Interactions

Cite this: DOI: 10.1039/xoxxoooooox

Man Yi Ho[a], Sarah Goodchild[b], Pedro Estrela[a,c], Daping Chu[a], Piero Migliorato[a,d]

Received ooth January 2012,
Accepted ooth January 2012

DOI: 10.1039/xoxxoooooox

www.rsc.org/

Detection of specific protein analytes is a technique widely used in disease diagnosis. Central to this approach is the fabrication of a sensing platform displaying a functional recognition element specific for the analyte targeted for detection. The most commonly utilised type of recognition element used for this purpose are antibodies, However direct generation of surfaces with high functional binding activity when using antibodies frequently presents a challenge, due to the conformational changes undergone by these molecules when physisorbed on a solid surface and/or variable activity when immobilized by covalent coupling techniques. Here, we present a novel label-free protein sensing platform based on a simplified and standardized immobilization process. The platform consists of self-assembled redox protein; Azurin (Az), that acts as scaffold, while sensing specificity is achieved through receptors that are coupled with chemical groups available on the surface of the Az protein. The redox activity of the Az within the sensing surface enables a label-free electrochemical detection method that can be readily miniaturized. We have observed a significant change in the electrochemical characteristic of the assay, upon a specific molecular interaction. A new model is also developed that can aid the future development of redox based bio-sensing techniques.

One of the consistent challenges remaining in the development of specific, high sensitivity platforms for biological sensing is the integration of recognition elements into the sensing surface used to provide the transduction signal. Antibodies, whilst providing a robust binding molecule, provide a challenge to the development of consistent biosensor surfaces due to direct immobilsation frequently exhibiting unpredictable changes in function depending on the sensor substrate material in combination with immobilization mechanism used (i.e. physisorption, chemical conjugation and choice of chemical conjugation type used) [1-3]. Generic mechanisms of linking transduction of molecular binding events to a sensor platform therefore remain of interest in the development of sensor platforms.

Adsorbed, redox active Self-Assembled Monolayers (SAMs) on metal have attracted considerable research efforts in the past two decades[4-10]. Recently, in addition to providing a model system for investigating interfacial electron transfer processes, redox active SAMs have found a new application in biomolecular detection by monitoring changes in the electrochemical environment of ferrocene-SAMs upon biomolecular interaction[11]. The challenge in such application is the implementation of a controlled immobilization process for the detection platform. This is especially difficult in the case of protein sensing because proteins have a complicated structure and can change folding depending on the environment. As a result, the platform has to be tailor-made to a particular target. In our approach, receptors are coupled to a scaffold consisting of the redox metalloprotein, Azurin (Az). This scaffold enables a standard self-assembled process whereas the specificity is provided by coupling different receptors to the Az. Furthermore, the scaffold protein provides redox activity enabling label-free detection. For the first time, we observed a significant switching of electrochemical characteristics of the SAM upon specific biomolecular interactions, which can be used as the basis of a novel mechanism for interrogating biomolecule detection.

Az is a metalloprotein which contains a copper ion cofactor that is bound by five amino acids[12]. The natural function of Az is to mediate electron transfer in denitrifying bacteria, but an increasing number of applications in molecular electronics are reported[13-18]. By exploiting the Cys3-Cys26 disulfide bond on the Az, a compact and highly ordered Az self-assembled monolayer can be formed on Au. Thiolated polyethylene glycol (PEG), which has been shown to reduce non-specific electrochemical signals in complex samples[19], is then used to passivate the remaining bare Au sites of the electrode, as shown in Figure 1a. When adsorbed onto the electrode, the copper ion can exchange electrons with the underlying electrode. To demonstrate the

applicability of the platform towards protein sensing, biotin was coupled to Az via accessible amine groups present on the Az protein (Figure 1b) using a simple amine coupling chemistry. This provides a simple model system for the investigation of the effects of protein binding through the use of Streptavidin as a model analyte. The coverage of the biotinylated Az on gold substrate was characterized with Quartz Crystal Microbalance (QCM), yielding an approximate coverage of 4.6 x 10^{12} cm^{-2}. This is of the same order of magnitude as the theoretical maximum coverage assuming Az has a circular shape of diameter 5.5 nm. The binding of the Streptavidin with the biotinylated Az platform was monitored with AC voltammetry, Electrochemical Impedance Spectroscopy (EIS) and also carried out in real time with QCM. (Please refer to the supporting information for the QCM measurements.)

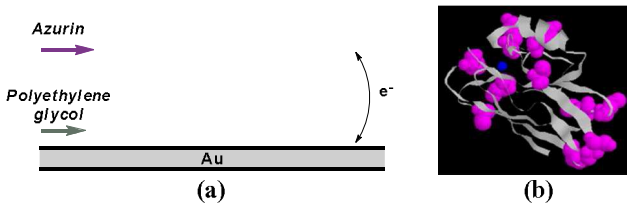

Figure 1 (a) Schematic representation of the Azurin monolyer (b) Structure model of Azurin. The lysine residues targeted by the amine coupling chemistry during biotinylation are shown highlighted in pink

The theoretical analysis of a redox SAM for biosensing applications has been previously carried out[8]. The governing equations of the system are:

$$E = E^{o'} + \left(\frac{RT}{nF}\right)\ln\left[\frac{\Gamma_O}{\Gamma_R}\right] \quad (1)$$

where $E^{o'} = E^{o} + \phi_{PET} - \phi_S$

$$\phi_{PET} - \phi_S = \frac{2RT}{zF}\sinh^{-1}\left[\frac{\sigma_M + \sigma_{PET} + \sigma_{Az} + \sigma_{target}}{\sqrt{8RT\varepsilon_o\varepsilon_3 c_{el}}}\right]$$

$$\sigma_M = \frac{\varepsilon_o\varepsilon_1}{d_1}\left[E^{o} + (\phi_{ref} - \phi_S) - \left(\frac{RT}{nF}\right)\ln\left(\frac{1-f}{f}\right)\right]$$

$$\sigma_{PET} = F\Gamma_T[z_O f + z_R(1-f)] \quad (2)$$

E, E^o and $E^{o'}$ are the applied potential, the standard electrode potential and the formal potential, respectively. ϕ_M, ϕ_{PET}, ϕ_S and ϕ_{ref} are the potentials at the metal, the plane of electron transfer (PET), the bulk solution and the reference electrode, respectively. The buffer solution has a dielectric constant ε_3 and electrolyte concentration of c_{el}. R, T, n and F are the molar gas constant, the absolute temperature, the number of electrons involved in the redox reaction and the Faraday's constant. σ_M, σ_{PET}, σ_{Az} and σ_{target} are the surface charge densities on the electrode, PET, azurin and the target protein, respectively. Γ_T, Γ_O and Γ_R are the total, oxidized and reduced redox molecules surface densities, $f = \Gamma_O/\Gamma_T$, z_O and z_R are the charge of the oxidized and reduced redox molecules. The SAM has a dielectric constant of ε_1 and a height of d_1.

The parameters of interest are the charge of the target (σ_{target}), and the electrolyte ionic strength. The dependence of the formal potential on these parameters is shown in Figure 2. There are two important features. Firstly, at a fixed ionic strength, the formal potential shows directional shifts depending on the sign and magnitude of σ_{target}. In other words, the formal potential reveals the change in the charge environment near the PET. This was experimentally observed in previous work on Ferrocene redox SAM[8], where the charge near the PET was manipulated by neutralization of either positively charged or negatively charged functional groups within the SAM. The directional shifts in the formal potential are measured by AC voltammetry. Secondly, the dependence of the formal potential on ionic strength is reversed when σ_{target} reaches a critical value. This can be seen from Equation (2): when $\sigma_M + \sigma_{PET} + \sigma_{Az} + \sigma_{target} > 0$, one would observe a reduction in the formal potential with increasing ionic strength, and vice versa for $\sigma_M + \sigma_{PET} + \sigma_{Az} + \sigma_{target} < 0$, one would observe an increase in formal potential with increasing ionic strength. The critical value hence lies at $(\sigma_{Az} + \sigma_{target}) = -(\sigma_M + \sigma_{PET})$ which is equal to -0.07 C m^{-2} in the case of Figure 2.

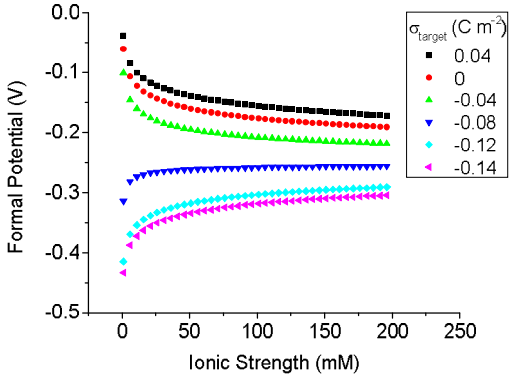

Figure 2 Theoretical calculations investigating the effect of ionic strength and the target charge on the formal potential. Input parameters are: E^o = -0.25 V, $(\phi_S - \phi_{ref})$ = -0.85 V vs Hg/Hg_2SO_4, ε_1 = 2.6, d_1 = 1.83 nm, $\Gamma_T = 1.4\times10^{-10}$ mol cm^{-2}, σ_{Az} = 0 and ε_3 = 78.5 (water)

Figure 3 shows the ionic strength titration experiments for the biotinylated Az, upon specific interaction with Streptavidin, and as a control, upon adding an antibody (an ovalbumin specific scFv-kappa fusion protein), and the specific reaction by adding Streptavidin. Formal potentials were extracted from AC voltammetry in pH7 phosphate buffer. It was observed that the formal potential increased with increasing ionic strength for both biotinylated Az and the control, whereas a complete opposite trend was present after specific reaction with Streptavidin. This is due to the positive charge carried by the Streptavidin. The fitted value of σ_{Az} = -0.031 C m^{-2}. After reacting with Streptavidin, the fitted value of $(\sigma_{Az} + \sigma_{target})$ = -0.022 C m^{-2}. Subtracting σ_{Az} from $(\sigma_{Az} + \sigma_{target})$ gives an estimated Streptavidin charge of +0.009 C m^{-2}. This positive charge of the Streptavidin is also confirmed by EIS measurements on the same electrode, as shown in Figure 3d. In the EIS, the measurement buffer contains a negatively charged redox couple, $[Fe(CN)_6]^{3-}$ and $[Fe(CN)_6]^{4-}$. Overcoming the potential barrier created by the SAM layer, the redox couple can exchange electrons with the underlying Au electrodes. This is characterized by the charge

transfer resistance (R_{ct}). After specific reaction with Streptavidin, a reduction in R_{ct} was observed, which suggests that Streptavidin has a net positive charge, therefore reducing the potential barrier for the negatively charged redox couple. The charge transfer resistance is reduced by 36kΩ.

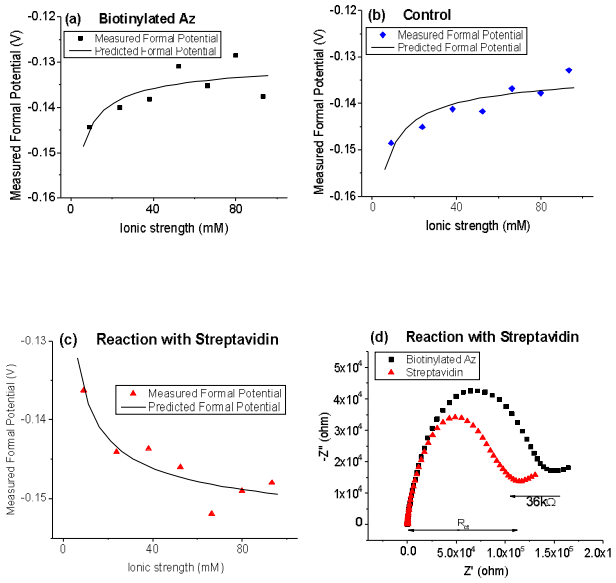

Figure 3 (a, b, c): Dependence of formal potential upon ionic strength: (a) biotinylated Az. For the predicted formal potential, the fitted parameters are E^o = -0.128V, σ_{Az} = -0.031 C cm^{-2}; (b) Control experiment of adding antibody to biotinylated Az. For the predicted formal potential, the fitted parameters are E^o = -0.131V, σ_{Az} = -0.031 C cm^{-2}. (c) Specific interaction with streptavidin. For the predicted formal potential, the fitted parameters are E^o = -0.155V, σ_{Az} + σ_{target} = -0.022 C cm^{-2}. Other input parameters are: $(\phi_S - \phi_{ref})$ = -0.85 V vs Hg/Hg_2SO_4, ε_1 = 20 (Az), d_1 = 5.5 nm (Az size), Γ_T = 7.6x10^{-12} mol cm^{-2} (from QCM) and ε_3 = 78.5 (water). (d) Electrochemical impedance spectroscopy of the same electrode used in (c).

The onset of the reversing trend happens at:

$$\sigma_{AZ} + \sigma_{target} > -(\sigma_M + \sigma_{PET})$$

In other words, the sensitivity of the platform is determined by -(σ_M + σ_{PET}). According to Equation (2), σ_{PET} is a function of the coverage Γ_T and f, and is calculated to be 0.0037 C m^{-2}, by taking Γ_T = 7.6 x 10^{-12} mol cm^{-2} from QCM measurements and f = 0.5 at the voltammetric peak. σ_M is 0.022 C m^{-2} also calculated from Equation (2), therefore - (σ_M + σ_{PET}) = -0.026 C m^{-2}. In the case of Figure 3, the above inequality is satisfied since σ_{Az} + σ_{target} = -0.022 C m^{-2}. To improve the sensitivity, one can minimize the dominating charge, σ_M, by increasing the distance between the PET and the electrode (d_1).

In conclusion, we have developed a novel protein sensing platform that allows simplification and standardization of creating different receptor layers by using a redox scaffold protein, Az. The applicability of the platform towards protein sensing was initially demonstrated with Streptavidin-Biotin interactions measured with QCM, EIS and AC voltammetry. The latter reveals a significant change of trend in the electrochemical behavior of the platform upon specific molecular interactions. On the basis of these results it is possible to envisage the described approach being extended to detection of additional protein analytes in a stepwise fashion using biotinylated recognition elements including antibodies. As such a novel type of label free electrochemically driven sensing platforms could be developed using the same approach.

Notes and references

[a] Electrical Engineering Division, Engineering Department, University of Cambridge, 9 J.J. Thomson Avenue, Cambridge CB3 0FA, UK
[b] Defence Science and Technology Laboratory, Porton Down, Salisbury SP4 0JQ, UK
[c] Department of Electronic & Electrical Engineering, University of Bath, Bath, BA2 7AY, UK (current address)
[d] Advanced Display Research Center and Department of Information Display, Kyung Hee University, Seoul 130-701, Korea

† Electronic Supplementary Information (ESI) available

1 A. K. Trilling, J. Beekwilder, H. Zuilhof, *Analyst*, 2013, **18**, 1619
2 S. L. Seurynck-Servoss, A. M. White, C. L. Baird, K. D. Rodland, R.C. Zangar, *Anal. Biochem.* 2007, **371**, 105
3 H. Xu, X. Zhao, J. R. Lu, D. E. Williams, *Biomacromolecules*, 2007, **8**, 2422
4 Chidsey, C. E. D.; Bertozzi, C. R.; Putvinski, T. M.; Mujsce, A. M., *J. Am. Chem. Soc.* 1990, **112**, (11), 4301
5 C. E. D. Chidsey, C. R. Bertozzi, T. M. Putvinski, A. M. Mujsce, *J. Am. Chem. Soc.* 2002, **112**, (11), 4301
6 S. E. Creager, G. K. Rowe, *J. Electroanal. Chem.* 1994, **370**, (1-2), 203
7 S. E. Creager, G. K. Rowe, *Anal. Chim. Acta* 1991, **246**, (1), 233
8 S. E. Creager, T. T. Wooster, *Anal. Chem.* 1998, **70**, (20), 4257
9 W. R. Fawcett, *J. Electroanal. Chem.* 1994, **378**, (1-2), 117
10 C. P. Smith, H. S. White, *Anal. Chem.* 1992, **64**, (20), 2398
11 M. Y. Ho, P. Li, P. Estrela, S. Goodchild, P. Migliorato, *J. Phys. Chem. B* 2010, **114**, (32), 10661
12 H. Nar, A. Messerschmidt, R. Huber, M. Van de Kamp, G. W. Canters, *J. Mol. Biol.* 1991, **221**, 765
13 S. U. Kim, J. H. Lee, T. Lee, J. Min, J. W. Choi, *J. Nanosci. Nanotechnol.* 2010, **10**, (5), 3241
14 S. U. Kim, A. K. Yagati, J. Min, J. W. Choi, *Biomaterials*, **31**, (6), 1293
15 T. Lee, W. A. El-Said, J. Min, B. K. Oh, J. W. Choi, *Ultramicroscopy* 2010, **110**, (6), 712
16 T. Lee, J. Min, S. U. Kim, J. W. Choi, *Biomaterials* 2011, **32**, (15), 3815
17 T. Lee, J. Min, J. H. Lee, J. W. Choi, *J. Nanosci. Nanotechnol.* **11**, (1), 523
18 E. D. Mentovich, I. Kalifa, N. Shraga, G. Ayrushchenko, M. Gozin, S. Richter, *Journal of Physical Chemistry Letters* 2010, **1**, (10), 1574
19 P. Estrela, D. Paul, P. Li, S. D. Keighley, P. Migliorato, S. Laurenson, P. Ko Ferrigno, *Electrochim. Acta* 2008, **53**, (22), 6489